Smart Structures and Systems, *Vol. 13, No. 3 (2014) 389-406*
DOI: http://dx.doi.org/10.12989/sss.2014.13.3.389

Optimal sensor placement for mode shapes using improved simulated annealing

K.H. Tong[1], Norhisham Bakhary*[1], A.B.H. Kueh[2] and A.Y. Mohd Yassin[1]

[1]Faculty of Civil Engineering, Universiti Teknologi, Malaysia, 81310 Skudai, Johor, Malaysia
[2]Construction Research Centre, Universiti Teknologi, Malaysia, 81310 Skudai, Johor, Malaysia

(Received October 30, 2012, Revised February 4, 2013, Accepted April 2, 2013)

Abstract. Optimal sensor placement techniques play a significant role in enhancing the quality of modal data during the vibration based health monitoring of civil structures, where many degrees of freedom are available despite a limited number of sensors. The literature has shown a shift in the trends for solving such problems, from expansion or elimination approach to the employment of heuristic algorithms. Although these heuristic algorithms are capable of providing a global optimal solution, their greatest drawback is the requirement of high computational effort. Because a highly efficient optimisation method is crucial for better accuracy and wider use, this paper presents an improved simulated annealing (SA) algorithm to solve the sensor placement problem. The algorithm is developed based on the sensor locations' coordinate system to allow for the searching in additional dimensions and to increase SA's random search performance while minimising the computation efforts. The proposed method is tested on a numerical slab model that consists of two hundred sensor location candidates using three types of objective functions; the determinant of the Fisher information matrix (FIM), modal assurance criterion (MAC), and mean square error (MSE) of mode shapes. Detailed study on the effects of the sensor numbers and cooling factors on the performance of the algorithm are also investigated. The results indicate that the proposed method outperforms conventional SA and Genetic Algorithm (GA) in the search for optimal sensor placement.

Keywords: optimal sensor placement; simulated annealing; coordinate-based solution coding

1. Introduction

The configuration of sensors is one of the most decisive factors in ensuring the reliability of modal data in vibration based structural health monitoring. However, the measurement of large civil structures at every degree of freedom (DOF) is impossible due to practical and cost constraints. Thus, the employment of an optimal sensor placement technique prior to the data acquisition stage is essential in obtaining outputs with heightened accuracy from a limited number of sensors.

Many quantitative methods for determining optimal sensor configuration have been developed for various engineering problems ranging from the analytical model updating of space stations to the health monitoring of civil structures. Studies related to optimal sensor placement have been performed across different engineering fields since the 1970s, the earliest approaches of which

*Corresponding author, Senior lecturer, E-mail: norhisham@utm.my

http://www.techno-press.org/?journal=sss&subpage=8 ISSN: 1738-1584 (Print), 1738-1991 (Online)

include the covariance matrix approach (Yu and Seinfeld 1973), model reduction method (Henshell and Ong 1974), kinetic energy method (KE) (Salama *et al.* 1987) and effective independence method (EfI) (Kammer 1990).

Although the optimisation methods for sensor placement appear to vary for different application types, most share the common objective of identifying structural dynamic behaviours as accurately as possible. Optimal sensor placement methods can generally be categorised into three major types according to their mechanisms of optimisation, which are i) direct ranking, ii) iterative expansion or elimination, and iii) discrete combinatorial optimisation.

To date, the direct ranking technique remains the fastest way of selecting optimal sensor locations where all approaches under this category rank every potential sensor location according to certain performance index, and the highest ranked sensor locations are chosen for the final layout. Some examples of this technique include the eigenvector product method (EVP) and the driving point residue approach (DPR). Recent applications of EVP and DPR in optimal sensor placement can be found in El-Borgi *et al*. (2008), Liu *et al*. (2008) and Meng *et al*. (2007). As attractive as their fast computation may seem, the main drawback of these techniques is that the sensor distribution tends to concentrate within a small range of DOFs due to the high function value at the optimal excitation points, as reflected in Meo and Zumpano (2005). Hence, these sensor configurations may not capture entire mode shapes accurately as a result of poor sensor distribution. The solution may also mislead the user when selecting the most appropriate sensor locations, especially when considering a finely meshed grid of sensor locations.

In the iterative elimination technique, every sensor location candidate is evaluated based on its contribution to a global performance index in a sequential manner, and the candidate that provides the smallest contribution is eliminated. This process is repeated until the number of candidates equals the desired number of sensors. On the other hand, expansion methods dictate that the sensor locations are gradually expanded to achieve the desired number of sensors. Typical examples of these techniques include the KE method and the EfI method as mentioned earlier. Li *et al*. (2007) compared the performance of both methods in determining the optimal sensor placement. The authors concluded that both methods provide an equal performance despite different sensor arrangements. Although the iterative expansion and elimination techniques are proved to be relatively fast in determining optimal solutions compared to the combinatorial optimisation technique, not many studies involving these techniques are able to provide highly accurate mode shape. This is due to their sub-optimal solutions which eventually lead to less accurate outcomes when identifying modal vectors. To overcome this problem, Li *et al*. (2012) proposed a new method by considering the dynamic characteristics and actual loading conditions of structure for the best modal and damage identification. Nevertheless, the authors suggested that further investigations need to be done to obtain a more conclusive assessment of the performance of the proposed method. Due to rapid development in modern computation, many researchers have applied heuristic algorithms to solve the sensor placement problem. Popular heuristic algorithms include simulated annealing (SA) (Kirkpatrick *et al*. 1983), tabu search (TS) (Glover and Laguna 1989, Glover and Laguna 1990), and genetic algorithm (GA) (Furaya and Haftka 1996, Ponslet *et al*. 1993). An early study of optimal sensor placement techniques in the field of vibration based damage detection has been presented by Worden and Burrows (2001). The authors have applied and compared the performance of SA and GA in determining optimal sensor placement by reducing a cost function, called the probability of damage misclassification. Using a plate structure that consists of twenty potential sensor locations, the authors have concluded that optimisation using SA is slightly better than GA in terms of the quality of sensor distribution. Since then, many improvements have been made in terms of the algorithms' performance, where most of them involve the improvement of GA, while efforts at fine-tuning the SA and other types of algorithms to address the sensor placement problem have been quite limited. For example, Guo *et al.* (2004) have implemented new strategies in GA to improve its convergence result, which involved improving the crossover operators and mutation process. The efficiency of the proposed method is demonstrated using the finite element model of a truss structure which consists of 14 nodes and 31 elements. Swann and Chattopadhyay (2006) have proposed a new optimisation procedure employing GA to detect arbitrarily located discrete delamination in composite plates using distributed piezoelectric sensors. GA was used to place sensors at the correct locations to detect both the presence and the extent of damage. Liu *et al.* (2008) have designed a forced mutation GA to improve the standard GA performance with a two dimensional array solution coding method for a truss structure. Cha *et al*. (2011) proposed an improved GA, which used the gene manipulation and multi-objective GA, to optimize the placement of sensors in frame structures to reduce active control cost and increase the structural control strategy's effectiveness. Although GA is demonstrated efficient in solving the problem of sensor placement, it is very time consuming due to complex optimisation process as a result of repeated evolution of the objective function and the population based nature of the search. Such disadvantage becomes more obvious when structures with many degrees of freedom are involved. Thus, in most cases, the number of sensor locations that is used to demonstrate the efficiency of GA has been relatively small. Attempts to overcome the problem of convergence time in GA include particle swarm optimisation (PSO) (Rao and Anandakumar 2007), virus evolution theory (Kang *et al*., 2008) and monkey algorithm (Yi *et al*. 2012). However, the application of these methods to vibration based health monitoring of civil structures is quite limited.

Because high efficiency is the utmost requirement in sensor placement, this study presents an improved SA algorithm to remedy the sub-optimal issues in the existing simple iteration methods. The algorithm is developed based on the sensor locations coordinate system to allow for searches in multiple dimensions rather than the one-dimensional searches available in conventional encoding methods. By performing simultaneous searches in multiple dimensions, the algorithm is capable of providing a better combination of sensor configurations while minimising iteration time. This study also introduces a normalised acceptance function to generalise the probability of accepting bad solutions at objective function values with different orders of magnitude. A numerical slab model with two hundred sensor location candidates is used to demonstrate the effectiveness of the proposed method. The results show that the proposed method significantly improves the optimisation of the objective functions compared to other methods. The results are also compared with the optimisation performance of a standard GA, and the determinant of the Fisher information matrix (FIM), the modal assurance criterion matrix (MAC), and the sum of the mean square errors of mode shapes (MSE) are applied to produce different optimal solution designs. Lastly, the difference between the finite element mode shapes and sensor placement interpolated mode shapes are calculated to evaluate the accuracy of the solutions obtained using different objective functions.

2. Simulated Annealing algorithm

2.1. Basic Concept

The combinatorial problem of sensor placement can be expressed as “finding the best possible combination of *r* sensors from *n* potential locations”. When the order of the sensor locations is not the main consideration, the number of possible combinations is idealised as $n!/r!(n-r)!$. The most direct approach to identify the best combination of sensor locations is by a random search, from which the solutions are generated and evaluated arbitrarily. However, this approach is inefficient due to the fact that the information learned from a given search is not utilised in future searches. Therefore, a modern heuristic algorithm such as SA is utilised to estimate the best solution.

The basic concept of the SA algorithm is based on the study by Metropolis *et al.* (1953) and addressed by Kirkpatrick *et al.* (1983) on combinatorial optimisation problems. Conceptually, the SA algorithm is analogous to the physical process of annealing, where a material is re-heated to its melting point and subjected to a controlled cooling process that recrystallises its microstructure formation, eventually improving the material’s properties. Similarly, the ultimate goal of the SA algorithm is to determine a global optimal solution to a problem that is governed by an objective function. Fig. 1 shows a typical flow diagram of the SA algorithm.

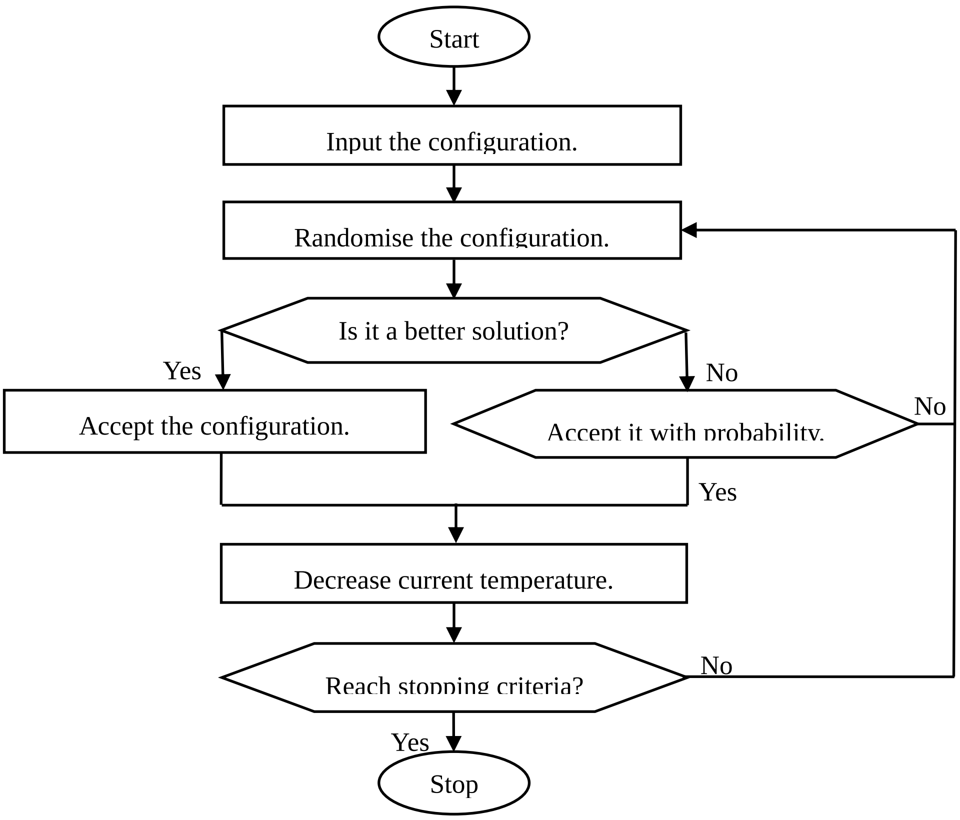

Fig. 1 Basic flow diagram of the SA algorithm

The optimisation process begins with a predefined initial sensor configuration. From this configuration, the algorithm then randomly finds a new configuration in the vicinity of its neighbours. The radius of the random search is proportional to the annealing temperature at that time. Normally, the newly generated solution is constrained by a set of boundary conditions such as the upper and lower bounds. Next, this solution is compared to the previous configuration based on the objective function value. The better solution is always accepted, while the weaker solution is accepted only if a randomly generated number [0, 1] is greater than a probability value p as given in Eq. (1)

$$p = \exp(-\mathrm{d}E/T) \tag{1}$$

where dE is the change in the objective function value and T is a temperature parameter that has the same unit as the objective function. Instead of accepting only the good solutions, it may consider a weaker solution to avoid becoming trapped within a local minimal region. The values of acceptance probability are close to 1 during the initial state when the temperature is high. Eventually, as the iteration proceeds and the temperature decreases, the value of acceptance probability approaches zero, indicating a low probability of accepting weak solutions.

The high temperature at the early stage in SA optimisation offers the capability of identifying the global optimal solution's rough features. As the annealing temperature decreases with the random search distance, the rough feature of the solution is then refined. This process is continued until the temperature reaches a minimum at which the entire system is frozen or, in the case of optimisation, the optimum configuration is found.

2.2 Improved solution encoding method

The solution coding method is an essential communication tool for an algorithm to record information regarding the placement of sensors in optimisation iterations. When applying SA to an optimisation problem, the design of the neighbourhood structure is important because the neighbourhood ranges can significantly affect the accuracy of the solutions (Miki *et al*. 2006). The most common type of coding for multivariable problems is binary code, as shown in Table 1(a), where n_l denotes the total number of potential locations. This binary code defines the sensor location as a binary string, in which '1' indicates that a sensor is available and '0' indicates otherwise, as applied in Worden and Burrows (2001), Guo *et al*. (2004), Liu *et al*. (2006). In this method, the sensor configurations are arranged in ascending order by node number, which is represented in the decimal string format. A set of constraints is normally applied to prevent one or more sensors from appearing at the same location.

Table 1(a) Binary solution encoding method

Location	1	2	3	4	5	6	7	8	…	n_l
Availability	0	1	0	1	0	0	0	0	…	1

Table 1(b) Decimal solution encoding method

Sensor	1	2	3	4	5	6	7	8	…	n_s
Location	7	8	11	12	42	44	46	75	…	79

Another alternative is to use a decimal solution encoding method in SA (DSA) as shown in Table 1(b), where n_s denotes the total number of sensors. The application of such a method to GA and PSO algorithms has been performed by Rao and Anandakumar (2007) and also Liu *et al* (2008), respectively. The disadvantage of these methods is that the search procedure is performed in a one-dimensional format, thus the SA's search space is limited to either the longitudinal or transverse directions as shown in Figs. 2(a) and 2(b). As a result, the search is unable to evaluate the complete combination of sensor locations, which substantially increases the computation time to find a global optimal result.

(a) Configuration 1

(b) Configuration 2

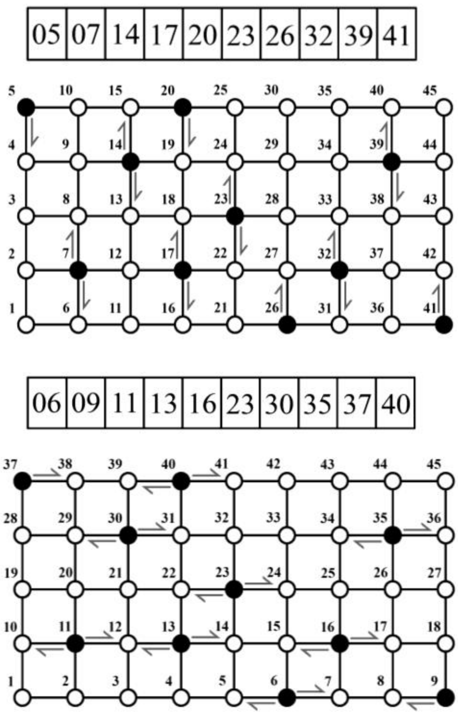

Fig. 2 Random search procedure in the DSA algorithm: (a) transverse random search in sensor configuration 1 and (b) longitudinal random search in configuration 2

This study proposes the use of a SA with a coordinate-based solution encoding (CSA) to overcome the issue of less spatial information encountered in conventional one-dimensional solution encoding. The basic concept of the CSA is to apply a random search of sensor points based on the geometry of the structure, which is performed by allowing the search procedure to move according to the actual coordinate system. To this end, a set of coordinate parameters (x_i, y_i and z_i) are assigned to each individual sensor and the next solution is determined by x_i+dx, y_i+dy and z_i+dz, where dx, dy, and dz, are the random search distances of the ith sensor. Fig. 3 illustrates the CSA method in two dimensions, in which 10 sensors are initially placed at nodes 5, 7, 14, 17, 20, 23, 26, 32, 39, and 41 together with their coordinate values, such as x_i, y_i and z_i. In this way, the next set of sensor configurations is randomly generated based on the coordinate values, such as x_1+dx, y_1+dy for the sensor at node 5 and x_2+dx, y_2+dy for the sensor at node 7, rather than using the DSA that gives $5+dx_1$ for the sensor at node 5 and $7+dx_2$ for the sensor at node 7.

Configuration 3

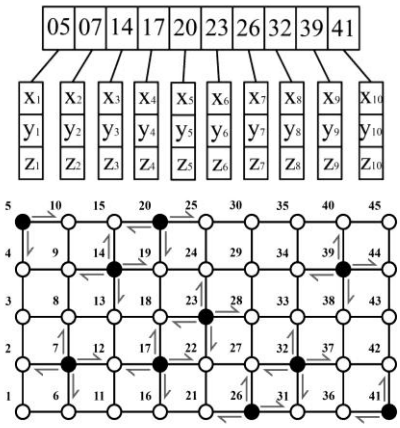

Fig. 3 Optimal sensor configuration search for the CSA algorithm in a 2D structure

---

Set objective_function (i.e., determinant of Fisher information matrix)

Set parameter n, N, T_0 and α; where n is number of sensors, N is number of potential locations, T_0 is initial temperature and α is the cooling factor

Set stopping_criteria (i.e., maximum iteration or minimum change in function value)

Initialise random sensor configuration in an ascending decimal format (X_i), which satisfies the inequalities $0 < X_i \leq N$ and $X_i \neq X_{i+1}$

Do until stopping_criteria is "yes"

Convert X_i to its coordinate matrix (X_{ijk})

Randomise X_{ijk} according to current temperature value

Convert X_{ijk} back to ascending decimal format, which satisfies the inequalities $0 < X_i \leq N$ and $X_i \neq X_{i+1}$

If the new function value is better than current function value

Acceptance "yes"

If the new function value is poorer than current function value

For exp (-dE/kT) > randomly generated number between [0, 1]

Acceptance "yes"

Else

Acceptance "no"

Decrease the current temperature by multiplying it with the cooling factor (α)

Fig. 4 CSA algorithm pseudo-code for sensor placement problem

As a result, CSA allows the sensor search procedure to move in all directions simultaneously instead of limited to vertical or horizontal direction as in the DSA method. Moreover, CSA has a better chance of avoiding premature convergence of the sensor configuration, especially towards the end of the algorithm when the temperature parameter is small, increasing the efficiency of determining the best sensor combination. The CSA algorithm's pseudo-code is given in Fig. 4 for ease of reproduction.

2.3 Normalised acceptance function

The acceptance function in SA controls the probability of accepting a bad solution p and the distance of the random search D. The Boltzmann's constant k is normally excluded from the acceptance function. In this way, the acceptance function does not work unless one of its parameters is normalised to make the ranges fall within the same order of magnitude. Therefore, the common approach in maintaining this balance is to assign an initial temperature equal to a randomly generated objective function value, as applied in Worden and Burrows (2001).

In classical combinatorial problems such as the Travelling Salesman problem, the issue in implementing the SA algorithm that is mentioned above, does not exist because the objective function E, temperature T, and random search distance D are applied using the same unit, which is the distance travelled. However, in the situation where E and T do not have the same unit as D, a normalisation factor must be introduced for either E and T or T and D to produce output values with the same unit. This leads to the proper transition of acceptance function values. Therefore, this paper considers a normalisation factor (k) in calculating the acceptance function value (P_n) as given in Eq. (2)

$$P_n = exp\ (-dE_i/kT_i) \tag{2}$$

where $k = E_0/T_0$, E_0 is the randomly generated objective function value and T_0 is the initial temperature. Hence, parameter T can be made equal to D without necessarily having the same unit as E due to the normalisation of dE and T by E_0 and T_0, respectively. With this approach, the acceptance function is applicable to all ranges of objective functions with different k values for different numbers of sensors.

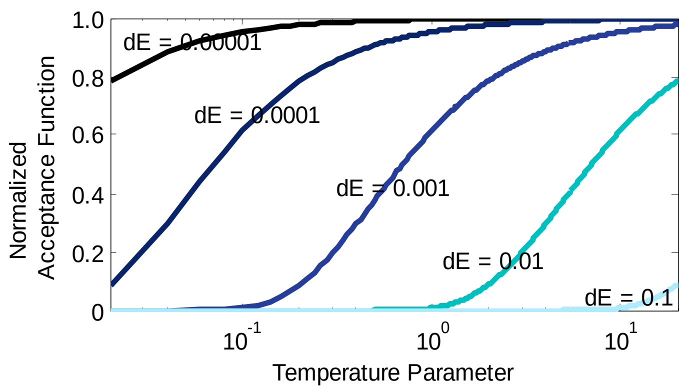

Fig. 5 Probabilities of the normalised acceptance function

Because good convergence characteristics in SA require the proper transition of the acceptance function, from random search behaviour (P_n =1) to greedy search behaviour (P_n =0), it is necessary to verify the proposed normalised acceptance function with respect to temperature and change in objective function value. For this reason, the acceptance function versus exponential temperature updates at specific values of the change in objective function is given in Fig. 5, which shows that the acceptance function values change from 1 to 0 smoothly. For example, the acceptance function values transition in a smooth s-shape from 1 to 0 when the change in the objective function value equals 0.001. Hence, appropriate SA convergence characteristics can be assured by applying the normalised acceptance function.

2.4 Geometric cooling schedule

The maximum search distance for a given number of sensors can be estimated by a priori knowledge of the average distance between the uniformly distributed sensors on the structure. Therefore, the initial temperature can be computed using the ratio of the total potential location to the given number of sensors. This process can substantially reduce computation time by avoiding excessive random searches during the early optimisation stage. A direct temperature update function is applied for this purpose, where the temperature parameter decreases exponentially with the increasing iterations and a corresponding cooling factor (α) as given in Eq. (3)

$$T_{n+1} = \alpha T_n \tag{3}$$

where T_n is the temperature at the nth iteration.

3. Objective functions

Three objective functions are applied in this study to obtain different optimal design of sensor configurations. The first criterion is based on the determinant of the Fisher information matrix (FIM) as given in Eq. (4), where the ϕ represents the modal vectors partitioned to the sensor locations. This criterion is applied because it is popularly employed for optimal sensor placement to measure the contribution of each sensor location to the linear independence of the target modes (Kammer and Yao 1994). Another importance of FIM determinant is to obtain sensor locations that provide the best estimate of damage coefficients (Guo *et al*. 2004). Studies that applied FIM-based criterion can also be found in Meo and Zumpano (2005) and Rao and Anandakumar (2007), and Stephan (2012).

$$FIM = |\phi^{\mathrm{T}}.\phi| \tag{4}$$

The second objective function aims to maximise the sum of orthogonality of modal vectors uses modal assurance criterion (MAC). This is because the MAC is the scalar constant that is used ideally to measure the correlation between mode shapes. Thus, many combinatorial sensor optimisation studies applied MAC as the objective function, for examples, in Rao and Anandakumar (2007), Liu *et al*. (2008) and Yi *et al*. (2012). In the current content, the second objective function applied in this study aims to maximise sum of MAC over the target modes as written in Eq. (5), where ϕ_{FE} is the finite element mode shapes, ϕ_{SP} is the sensor placement mode shapes and m denotes the number of target modes. Since the mode shapes data obtained from sensors are not complete to construct ϕ_{SP}, the cubic interpolation technique is used to estimate the incomplete data based on the measured data from limited sensor locations. Thus, ϕ_{SP} is obtained based on a combination of the interpolated mode shape values and the measured mode shape values. The cubic interpolation technique is chosen because it can provide a set of smooth curves that closely approximates the actual mode shapes using limited data. The cubic interpolation is also applied in Meo and Zumpano (2005) to obtain the complete mode shapes from the data of structure at selected sensor locations.

$$MAC = \sum_1^m \frac{|\phi_{FE}^T . \phi_{SP}^T|^2}{\phi_{FE}^T \phi_{FE} . \phi_{SP}^T \phi_{SP}} \tag{5}$$

The third objective function used in the optimisation works is by minimising the mean square errors (MSE) between the two modal vectors, ϕ_{FE} and ϕ_{SP}, as described above. The optimisation concept of MSE is similar to MAC, which is to measure the quality of sensor placement generated mode shapes. However, MSE measures the quality of sensor placement mode shapes in a more direct manner, making the calculation of objective function value relatively faster. Hence, the third objective function that used in this study is the sum of MSE over the target modes and is given in Eq. (6), where *n* represents the total number of sensor locations.

$$MSE = \sum_1^m \frac{\sum_1^n |\phi_{FE} - \phi_{CI}|^2}{n} \tag{6}$$

In addition to the above optimal criteria, there are also other alternatives for optimising the sensor locations. For examples, the objective functions that based on modal kinetic energy and modal strain energy, as also applied in Rao and Anandakumar (2007) and Liu *et al.* (2008), respectively. However, these criteria are similar to FIM determinant criterion, but those objective functions require extra input parameter, such as the global mass matrix and global stiffness matrix to perform the optimisation. For comparison purpose, therefore, only the FIM determinant, MAC and MSE objective functions are applied the present study.

4. Numerical example

4.1 Finite element model

A numerical model of a rectangular concrete slab is used to demonstrate the efficiency of the proposed method. The slab is 7.0m long, 2.7m wide and 0.2m thick and it has an elastic modulus of E= 22.5 GPa, a mass density of ρ= 2450 kgm^{-3}, and a Poisson's ratio of r = 0.15. 200 active nodes are selected as potential sensor locations. The analysis considers the first three vertical bending modes for demonstration purposes as illustrated in Fig 6, the natural frequencies of which are 41.95, 164.24 and 357.44 Hz, respectively.

4.2 Performance analysis

The results of decimal solution encoding (DSA) and coordinate-based solution encoding (CSA) are compared using 10 sensors with identical random initial configurations and a cooling factor of 0.97. Figs. 7(a)-7(c) shows the comparison of the results using the three different objective functions, respectively. These results show that CSA provides a better convergence rate than DSA. For example, the FIM values obtained with CSA in Fig. 7(a) are higher than those obtained with

DSA during most of the iterations. This trend becomes consistent especially after 300 iterations, indicating that DSA locates the optimal sensor points more efficiently than DSA. Similar results are observed in Fig. 7(b), where the comparison of both encoding methods using the sum of the MAC values is presented. As the iteration proceeds, the proposed CSA method gives better objective function values than DSA in most of the iterations. The high MAC value indicates that the corresponding solution is more accurate at identifying the modal vectors. The same type of performance is identified in Fig. 7(c), where the sum of the MSE between two mode shapes plot is minimised. It is also noted that the MSE function values for CSA are lower than those for DSA, indicating that CSA is capable of providing lower estimation errors than DSA. In conclusion, CSA is found to be relatively superior at searching for the best sensor configuration.

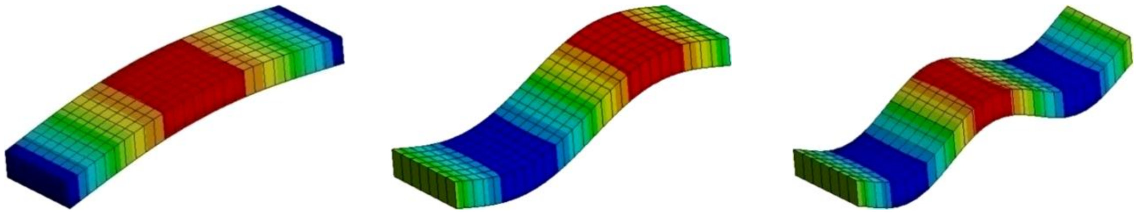

Mode 1 Mode 2 Mode 3

Fig. 6 The first three vertical bending modes of the slab

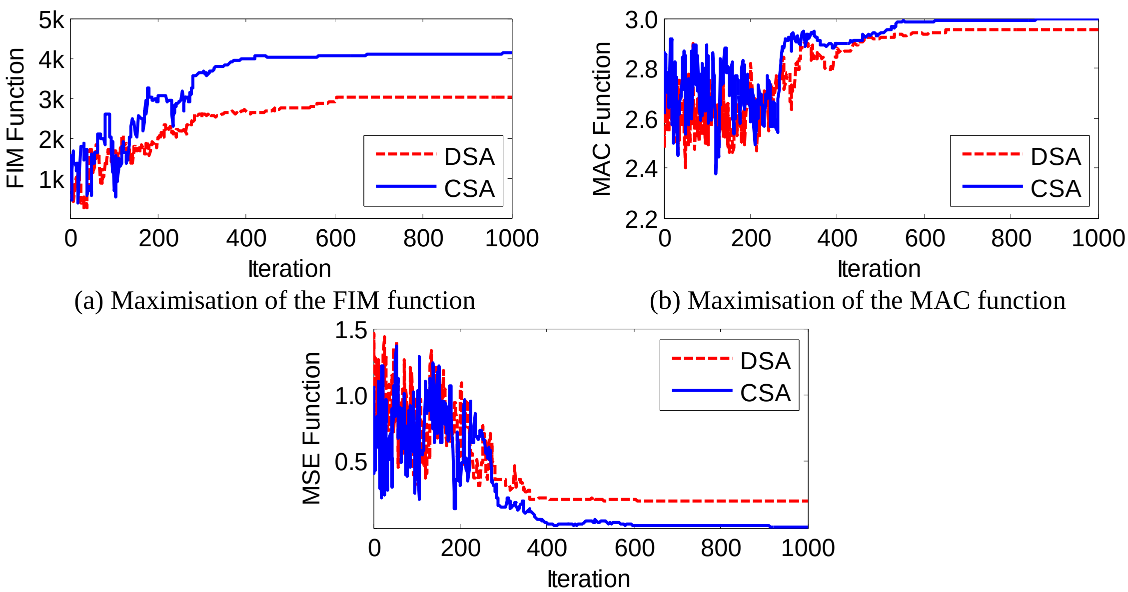

(a) Maximisation of the FIM function

(b) Maximisation of the MAC function

(c) Minimisation of the MSE function

Fig. 7 Convergence curves obtained with DSA and CSA using three different objective functions

Table 2 Comparison of DSA, CSA and GA performance for different computation times

Algorithm	Parameter		Period	Optimal sensor configuration	Function value
DSA	α	0.97	60 sec.	16 31 36 41 56 73 76 88 156 191	2.31
		0.997	300 sec.	9 23 52 65 80 92 121 136 164 200	2.60
		0.999	600 sec.	11 56 65 84 104 121 148 160 169 200	2.54
CSA	α	0.97	60 sec.	33 34 37 40 97 101 104 153 157 168	2.95
		0.997	300 sec.	33 36 39 80 97 101 152 153 157 169	2.84
		0.999	600 sec.	33 36 39 40 92 104 105 156 160 161	2.95
GA	s	5	60 sec.	40 57 58 78 90 96 97 141 154 184	2.42
		29	300 sec.	29 34 56 89 109 112 160 161 170 173	2.78
		60	600 sec.	25 31 36 88 89 109 168 169 170 173	2.82

The optimisation performances of DSA, CSA and the standard GA are investigated to further demonstrate the applicability of the proposed method. Both SA methods (DSA and CSA) and the GA are executed for specified computation times to evaluate their performance in maximising the MAC function for a distribution of 10 sensors. The GA parameters applied in this study are elite count = 10% of the population size, crossover fraction = 0.7 and mutation rate = 10%. The test is carried out in three parts by varying the computation time between 60 seconds, 300 seconds and 600 seconds. To compromise the specified computation time using SA and the GA, the cooling factors (α) of the SA and the population size (s) of the GA are randomly adjusted to achieve complete convergence of the solution before the given periods, respectively. A summary of the best objective function values obtained with DSA, CSA and the GA is given in Table 2. The results show that the MAC values of CSA are higher than those generated by DSA and the GA. It is also observed that CSA produces more consistent sensor placement than DSA and the GA, where the sensor configuration is almost similar at different computation times. Hence, CSA is evidently capable of providing better optimisation performance than DSA and the GA.

4.3 Effect of the number of sensors

In sensor placement optimisation, a larger number of sensors requires a longer function convergence time. Therefore, it is useful to explore the characteristics of convergence for different objective functions with different numbers of sensors. Three different quantities of sensor, 10, 15 and 20, are used for this purpose. Fig. 8(a) shows the convergence results for DSA and CSA in terms of the FIM values for different numbers of sensors. The results show that the convergence delays as the number of sensors increases. For example, CSA converges at approximately 100 iterations when 10 sensors are used, while 500 and 1500 iterations are required for 15 and 20 sensors, respectively, indicating that a higher number of sensors requires a longer convergence time. Similar trends are also observed when using MAC and MSE as the objective functions, as shown in Figs. 8(b) and 8(c), respectively, where a higher number of sensors introduces a higher number of variables into the optimisation process and thus requires a longer convergence time to obtain the optimal function values. The results also show that CSA provides more accurate results than DSA for the different numbers of sensors in terms of all three objective functions. For example, in Figs. 8(a) and 8(b), the FIM and MAC values obtained using CSA using 10, 15 and 20 sensors are significantly higher than those produced with DSA. The same situation occurs in Fig. 8(c), where the MSE values using CSA and three different numbers of sensors are lower than those obtained using DSA, indicating that the CSA produces relatively less error.

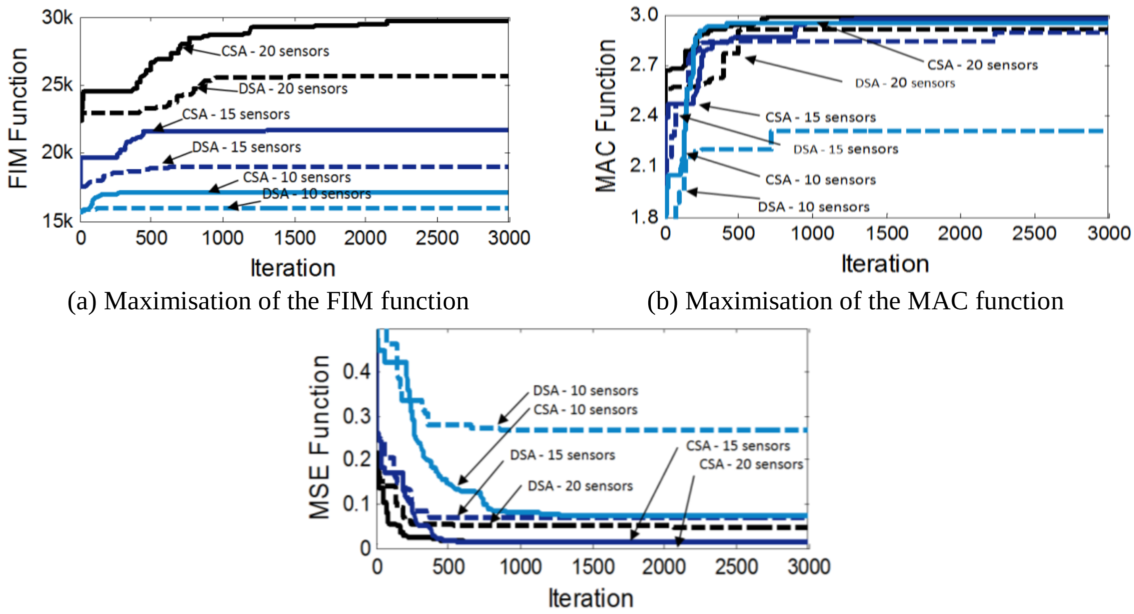

(a) Maximisation of the FIM function (b) Maximisation of the MAC function

(c) Minimisation of the MSE function

Fig. 8 Convergence curves using DSA and CSA and different numbers of sensors

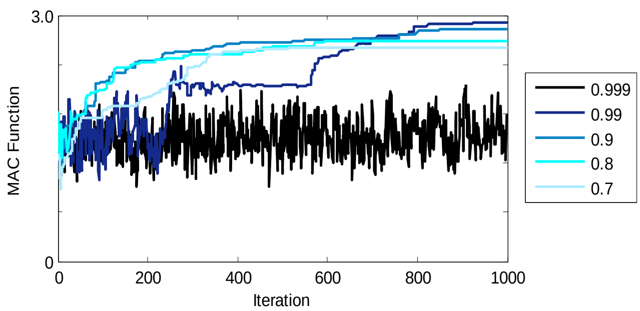

Fig. 9 CSA optimisation using different cooling factor values.

4.4 Effect of the cooling factor

In SA, the quality of the solution is highly dependent on the cooling factor value. For example, a rapid cooling process dictates that the algorithm converge after a very short period of time, while the opposite is true for a slow cooling process. Therefore, a sensitivity test is performed to examine the effects of the cooling factor on the performance of the SA algorithm and to subsequently find the optimal cooling factor. The algorithm is executed at increasing cooling factor values of 0.7, 0.8, 0.9, 0.99 and 0.999, and the resulting convergence curves are shown in Fig. 9, which shows that the objective function values are relatively higher when the cooling factor is higher. For example, when maximising the MAC function value using cooling factors of 0.7, 0.8, 0.9 and 0.99, the best function values after 1000 iterations are 0.87, 0.90, 0.94 and 0.97, respectively. However, in the case of a cooling factor of 0.999, the function value experiences a large perturbation, requiring relatively more iteration convergence. Therefore, it is concluded that a higher cooling factor is needed to obtain a better optimisation result from the proposed algorithm, and the optimal cooling factor value is approximately 0.99.

4.5 Optimal sensor configurations

This section compares the optimal sensor configurations generated by the proposed CSA algorithm based on the three objective functions. Conceptually, for damage identification purpose, the optimum criterion should be related to maximum damage information indicating which sensor locations will have the highest sensitivity to potential damages to the structural system, as proposed by (Xia and Hao 2000). However, this aspect is not considered in this study. Figs. 10(a)-10(c), 11(a)-11(c) and 12(a)-12(c) show the best configurations for 10, 15 and 20 sensors using FIM, MAC and MAC as the objective functions, respectively. When employing the FIM objective function with 10, 15 and 20 sensors, it is observed that the sensors are clustered around several regions of high excitation along the longitudinal edges, implying that although the FIM determinant value is high, the distribution of the sensors is inadequate for accurately capturing the modes of vibration, even though additional sensors are added. Such a distribution of the sensors is regarded as insufficient for detecting damage, especially local damage. A similar situation has been reflected in Meo and Zumpano (2005) when applying FIM-based methods (EfI and EfI with DPR) in their study. On the other hand, the optimal sensor distributions produced by the improved SA algorithm based on MAC and MSE, as shown in Figs. 11(a)-11(c) and 12(a)-12(c) are better distributed throughout the structure compared to the distribution created with the FIM objective function. These improved distributions allow the sensors to capture better vibration modes and provide more accurate damage detection. Based on the results obtained, it can be observed that the optimal sensor configurations of the three objective functions have significantly changed when more sensors were considered. This trend of results is obvious when applying the MAC and MSE objective functions. For example, the optimal position for 10 sensors may not applicable to 20 sensors, and vice versa. This is because, to obtain the best objective function values, the optimisation process needs to rearrange the sensor location which resulted in different configurations for different numbers of sensor.

The absolute differences between the finite element mode shapes (ϕ_{FE}) and the sensor placement mode shapes (ϕ_{SP}) obtained from the three objective functions are calculated to evaluate the accuracy of different objective functions in the optimisation of sensor placement using CSA. As mentioned earlier, the ϕ_{SP} is the estimated mode shapes based on the sensor points' data using cubic interpolation technique.. Tables 3(a)-3(c) displays the errors for the three objective functions under the corresponding target modes for the different numbers of sensor. Table 3(a) shows the calculated errors for FIM, MAC and MSE when 10 sensors are used in the sensor optimisation process. The comparison reveals that the FIM method gives higher error values than the MAC and MSE methods because FIM-based methods concentrate sensor positions in high excitation regions, such as at the peak values of mode shapes. The results also show that larger errors occur at higher modes with all three objective functions, indicating that higher modes of vibration contain larger mode shape interpolation errors. A similar trend occurs when the number of sensors is increased to 15 and 20, as shown in Tables 3(b) and 3(c). The results also show that the error between the actual mode shape and the interpolated mode shape decreases as the number of sensor increases.

Thus, more measurement points are required in practice to accurately capture the higher modes because they are more geometrically complex. Based on the results, it can be concluded that the MAC and MSE methods provide significantly smaller interpolation errors than the FIM method, and the MAC method slightly outperforms the MSE method when applied to a large number of sensors, especially in the case of higher number of sensor.

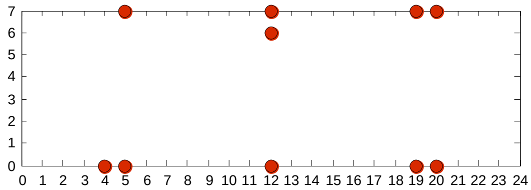

(a) 10 sensors

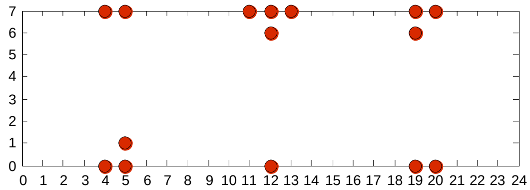

(b) 15 sensors

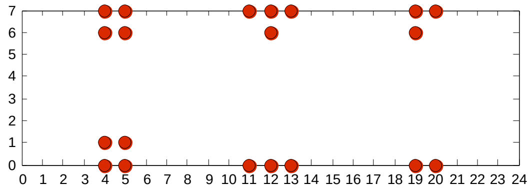

(c) 20 sensors

Fig. 10 Optimal sensor placements designed by the FIM objective function

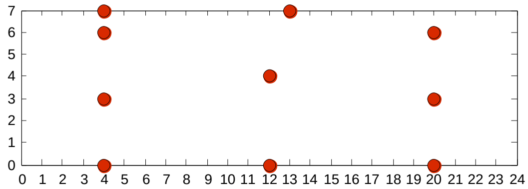

(a) 10 sensors

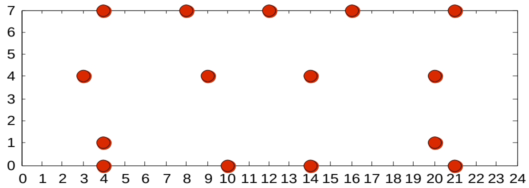

(b) 15 sensors

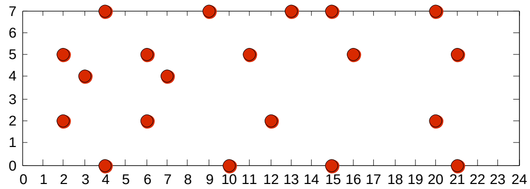

(c) 20 sensors

Fig. 11 Optimal sensor placements designed by the MAC objective function

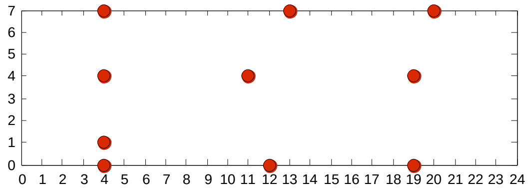

(a) 10 sensors

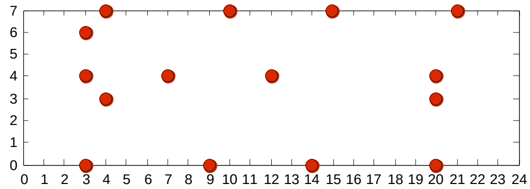

(b) 15 sensors

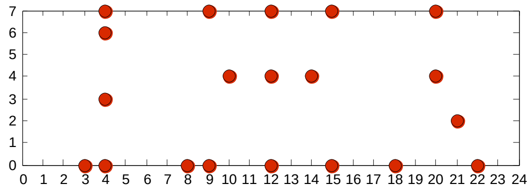

(c) 20 sensors

Fig. 12 Optimal sensor placements designed by the MSE objective function

Table 3(a) Absolute differences between the finite element mode shapes and sensor placement mode shapes for 10 sensors

Objective Function	Mode 1	Mode 2	Mode 3	Total
FIM	16.0603	137.3433	186.8573	340.2609
MAC	4.2236	37.557	43.7709	85.5515
MSE	2.9134	24.8512	34.4921	62.2567

Table 3(b) Absolute differences between the finite element mode shapes and sensor placement mode shapes for 15 sensors

Objective Function	Mode 1	Mode 2	Mode 3	Total
FIM	13.3993	101.807	136.2345	251.4408
MAC	1.7195	9.9212	20.0819	31.7226
MSE	2.4592	14.7618	21.4708	38.6918

Table 3(c) Absolute differences between the finite element mode shapes and sensor placement mode shapes for 20 sensors

Objective Function	Mode 1	Mode 2	Mode 3	Total
FIM	9.8462	63.5935	97.1403	170.5800
MAC	1.4543	9.0181	16.8573	27.3297
MSE	2.4173	11.6523	17.5037	31.5733

5. Conclusions

This paper presents a combinatorial optimal sensor placement technique based on the SA algorithm. Innovations in SA, such as coordinate-based solution encoding and the normalised acceptance function are introduced to improve the algorithm's performance. The values of the proposed encoding method are based directly on the exact coordinate system of the structure to overcome the issues encountered from having less spatial information in conventional 1D encoding methods. By using the proposed method, a realistic neighbourhood structure of sensor locations can be formed and improve SA's random search mechanism. A normalisation of probability acceptance function is introduced to standardise different ranges of objective function values and to ensure the proper convergence characteristics of SA.

The performance of two SA-based methods (DSA and CSA) and a GA-based method are investigated for specific computation times. The test results show that the proposed SA algorithm (CSA) is superior to DSA and the GA in terms of its objective function values. Adopting the proposed CSA as an optimisation template, three objective functions for optimal sensor placement are evaluated based on the absolute difference values between the finite element mode shapes and sensor placement mode shapes. This study finds that optimal sensor configurations designed by MAC and MSE functions have significantly smaller mode shape errors compared to those designed by the FIM function, and the MAC function shows slightly better performance when applied to a larger number of sensors.

Acknowledgments

This work was funded by the Ministry of Higher Education, Malaysia under Fundamental Research Grant Scheme (4F051 and 05H21) and Research University Grant Scheme (Q.J.13000.7122.01J99).

References

Cha, Y.J., Raich, A., Barosso, L. and Agrawal, A. (2011), "Optimal placement of active control devices and sensors in frame structures using multi-objective genetic algorithms", *Struct. Control Health Monit*., **20**(1), 16-44.

El-Borgi, S., Neifar, M., Cherif, F., Choura, S. and Smaoui, H. (2008), "Modal identification, model updating and nonlinear analysis of a reinforced concrete bridge", *J.Vib. Control*., **14**(4), 511-530.

Furuya, H. and Haftka, R.T. (1996), "Combining genetic and deterministic algorithms for locating actuators on space structures", *J. Spacecraft Rockets*, **33**(3), 422-427.

Glover, F. and Laguna, M. (1989), "Tabu search - Part I", *ORSA J. Comp*., **1** 190-206.

Glover, F. and Laguna, M. (1990), "Tabu search - Part II", *ORSA J. Comp*., **2** 4-32.

Guo, H.Y., Hang. L.Z., Zhang, L.L. and Zhou, J.X. (2004), "Optimal placement of sensors for structural health monitoring using improved genetic algorithms" , *Smart Mater. Struct*., **13**(3), 528-534.

Henshell, R.D. and Ong, J.H. (1974), "Automatic masters for eigenvalue economization", *Earthq. Eng. Struct. D*., **3**(4), 375-383.

Kammer, D.C. (1990), "Sensor placement for on-orbit modal identification and correlation of large space structures" , *Proceedings of the 19th American Control Conference*, Califonia.

Kammer, D.C. and Yao, L. (1994), "Enhancement of on-orbit modal identification of large space structures

through sensor placement", *J. Sound Vib*., **171**(1), 119-139.
Kang, F., Li, J.J. and Xu, Q. (2008), "Virus coevolution partheno-genetic algorithms for optimal sensor placement", *Adv. Eng. Inform*., **22**(3), 362-370.
Kirkpatrick, S., Gelatt, C.D. Jr and Vecchi, M.P. (1983), "Optimization by simulated annealing", *Science*, **220**(4598), 671-680.
Li, D.S., Li, H.N. and Fritzen, C.P. (2007), " The connection between effective independence and modal kinetic energy methods for sensor placement", *J. Sound Vib*., 305(4-5), 945-955.
Li, D.S., Li, H.N. and Fritzen, C.P. (2012), "Load dependent sensor placement method: theory and experimental validation", *Mech. Syst. Signal Pr*., **31**(0), 217-227.
Liu, W., Gao, W.C., Sun, Y. and Xu, M.J. (2008), "Optimal sensor placement for spatial lattice structure based on genetic algorithms", *J. Sound Vib*., **317**(1-2), 175-189.
Liu, W., Hou, Z.K. and Demetriou, M.A. (2006), "A computational scheme for the optimal sensor and actuator placement of flexible structures using spatial measures", *Mech. Syst. Signal Pr*., **20**(4), 881-895.
Meng, X., Dodson, A.H. and Roberts, G.W. (2007), "Detecting bridge dynamics with GPS and triaxial accelerometers", *Eng. Struct*., **29**(11), 3178-3184.
Meo, M. and Zumpano, G. (2005), "On the optimal sensor placement techniques for a bridge structure", *Eng. Struct*., **27**(10), 1488-1497.
Metropolis, N., Rosenbluth, A.W., Rosenbluth, M.N. and Teller, A.H. (1953), "Equation of state calculations by fast computing machines", *J. Chem. Phys*., **26**(6), 1087-1092.
Miki, M., Hiwa, S. and Hiroyasu, T. (2006), "Simulated annealing using an adaptive search vector", *Proceedings of the IEEE Conference on Cybernetics and Intelligent Syst*., Bangkok.
Ponslet, E., Haftka, R.T. and Cudney, H.H. (1993), "Optimal placement of tuning masses on truss structures by genetic algorithms", *Proceedings of the 34th AIAA/ASME/ASCE/AHS/ASC Struct., Structl. Dyn. and Mater. Conference*, California.
Rao, A.R.M. and Anandakumar, G. (2007), "Optimal placement of sensors for structural system identification and health monitoring using a hybrid swarm intelligence technique", *Smrt. Mater. Struct*., **16**(6), 2658-2672.
Salama, M., Rose, T. and Garba, J. (1987), "Optimal placement of excitation and sensors for verification of large dynamical systems", *Proceedings of the 28th Struct., Structl. Dyn. and Mater. Conference*, California.
Stephan, C. (2012), "Sensor placement for modal identification", *Mech. Syst. Signal Pr*., **27**, 461-470.
Swann, C. and Chattopadhyay, A. (2006) "Optimization of Piezoelectric Sensor Location for Delamination Detection in Composite Laminates", *Eng. Opt*., **38**(5),511-528.
Worden, K. and Burrows, A.P. (2001), "Optimal sensor placement for fault detection", *Eng. Struct*., **23**(8), 885-901.
Xia, Y. and Hao, H. (2000), "Measurement selection for vibration-based structural damage identification", *J. Sound Vib*., **236**(1), 89-104.
Yi, T.H., Li, H.N. and Zhang, X.D. (2012), "A modified monkey algorithm for optimal sensor placement in structural health monitoring", *Smart Mater. Struct.*, **21**(10), 105033.
Yu, T.K. and Seinfeld, J.H. (1973), "Observability and optimal measurement location in linear distributed parameter systems", *Int. J. Control*, **18**(4), 785-799.

CC